



# Deposition Behavior and Characteristics of Cold-Sprayed Cu-Cr Composite Deposits

Xiang-kun Wu, Xiang-lin Zhou, Hua Cui, Xiong Zheng, and Ji-shan Zhang

(Submitted August 3, 2011; in revised form December 31, 2011)

**In order to explore the feasibility of cold spraying as method to prepare Cu-Cr composite, the deposition behavior was analyzed. The results show that particles parameters, such as morphology, size distribution and deformability, result in different deposition behavior. For Cu, since plastic deformation easily occurs, when a Cu particle impacts Cu substrate, both particle and substrate at the interface undergo extensive deformation, resulting in the greater bond probability. Although the velocity of Cr is higher than that of Cu, Cr particles have lower bond probability because of its hardness and fragility. Cr particles are embedded in the Cu particles. The properties of Cu-15%Cr meet industrial standard, superior to the composite prepared by explosive compaction. The results reveal cold spraying can be considered as a suitable technology for Cu-Cr composite.**

**Keywords** cold spray, composite deposits, Cu-Cr, deposition

## 1. Introduction

Cr particle-reinforced Cu matrix composite is also called Cu-Cr alloy, and it is a kind of pseudo-alloy where Cr particle embeds in Cu matrix. Different compositions of Cu-Cr have been widely used as electrical contact materials, especially in medium-voltage, high-current vacuum breakers because of its excellent electrical conductivity, high breaking current capability, and high capability of resistance electric arc corrosion and resistance surface fusion welding (Ref 1). Cu and chromium are immiscible, so they fully retain their good performance. Indeed, Cu has a relatively low melting point, high electrical conductivity and thermal conductivity and good plasticity, which will be helpful to improve the breaking current capability and ensure the large operating current in circuit breaker, while Cr with a relatively high melting point and the brittle nature provides a high voltage withstand property and anti-corrosion property of arcing. Also, the strong affinity of Cr and oxygen ensures a high degree of vacuum in the interrupter (Ref 2). High quality Cu-Cr alloy requires that Cr phase must uniformly distribute in Cu matrix, and the alloy should be dense. At present, there are several different methods to manufacture Cu-Cr bulk alloy, such as mixed powder sintering (Ref 3, 4), melt infiltration, arc melting,

rapid solidification (Ref 5, 6), thermal spraying (Ref 7) and explosive compaction (Ref 3). However, there are still problems regarding the preparation of Cu-Cr alloy, namely, the alloy is not dense, and the bond between the Cu matrix and the Cr particles is not strong, and as a result, the breaking capability and high voltage withstands property are reduced; in addition, high content of nitrogen and oxygen elements reduce the degree of the vacuum in interrupter; what's more, Cr phase is not uniformly distributed in the Cu matrix. Many researchers are devoted to improve the preparation process or explore the new technology in order to promote the materials properties to meet the higher requirements with the development of vacuum contact materials.

Cold gas dynamic spraying, simply called cold spraying, is a new coating process and manufacturing technology. This is a solid-state process because the temperature remains well below the melting temperature of the spray material. In comparing with thermal spraying, the coating quality is improved with dense layers, higher bonding force and lower oxidation (Ref 8). The cold-sprayed deposit retains the properties of the original powders because the particles only experience severe plastic deformation during impact (Ref 9, 10). Moreover, without melting and solidification, the deposits mainly exist in the form of compressive stress (Ref 11), so thick coatings or even bulk materials can be prepared. The preparation of metallic multi-component deposits by cold spraying, therefore, has been a research focus over the years. Numerous types of metallic multi-component materials have been successfully sprayed, such as W-Cu composite coating (Ref 12-14), Fe-Al (Ref 15), Ti-Al (Ref 16), Cu-Al<sub>2</sub>O<sub>3</sub> (Ref 17), and so forth. These reported results showed that a uniform coating with high density can be achieved by cold spraying under optimized processing parameters. Therefore, cold spraying may be a suitable method to produce high quality Cu-Cr composite. However, when mixed composite powders are used for the

Xiang-kun Wu, Xiang-lin Zhou, Xiong Zheng, and Ji-shan Zhang, State Key Laboratory for Advanced Metals and Materials, University of Science and Technology Beijing, Beijing 100083, China; and Hua Cui, School of Materials Science and Engineering, University of Science and Technology Beijing, Beijing 100083, China. Contact e-mail: wuxiangkun451@yahoo.com.cn.

feedstock, the differences in mechanical properties, physical properties, and particle sizes will inevitably result in different critical velocities and deposition behavior of each component, which affects the deposits properties.

In the present work, Cu-Cr composite deposit was prepared using a home-made cold spray system, and the deposition behavior and deformation of each component of mixed composite powders were analyzed to elaborate the deposit formation. Then the microstructure and the mechanical and electrical properties of the deposits were characterized.

## 2. Experimental Procedures

Cold-sprayed Cu-Cr deposits were prepared using a home-made cold spray system developed by the University of Science and Technology Beijing, China. The converging-diverging de-Laval nozzle with a round-type cross-section has a throat diameter of 3.8 mm and exit diameter of 7.8 mm. Nitrogen was used as the main process gas, and the process gas pressure and temperature were 2.0 MPa and 600 °C, respectively, and the gun standoff distance was 20 mm. The gun was fixed, the substrate was mounted on the numeric controlled X-Y-Z platform.

To observe particle/substrate interaction, single-particle impacts during spraying experiments were produced by the wipe-tests, in which a polished substrate is moved rapidly through the spray jet. During the wipe-tests, the powder feed rate was less than 5 g/min, and the traversal speed of the substrate was 3000 mm/min. When preparing the coatings, the traversal speed of the substrate was 600 mm/min with two passes. Table 1 summarizes cold-spraying parameters used in this study. Commercially available Cu powder and Cr powder were used as feedstock. The characteristic of the feedstock powders are listed in Table 2 and described in detail in “Characteristics of the Powders” section. Two powders were mixed for 2 h

**Table 1** Cold-spraying parameters used in this study

	Wipe test	Coating preparation
Process gas	N <sub>2</sub>	N <sub>2</sub>
Gas pressure, MPa	2.0	2.0
Gas temperature, K	873	873
standoff distance, mm	20	20
Traversal speed, mm/min	3000	600
Powder feed rate, g/min	<5	11
Gas mass flow rate, L/min	1700	1700
Spray pass	1	2

**Table 2** The characteristic of the feedstock powders used in cold spraying process

Powders	Composition	Nanohardness, GPa	D <sub>50</sub> , μm	Density, g/cm <sup>3</sup>	Loose density, g/cm <sup>3</sup>	Tap density, g/cm <sup>3</sup>	Carr index
Cu	>99.8%Cu	1.77 ± 0.12	25	8.96	5.02	5.79	90.5
Cr	>99.5%Cr	2.96 ± 0.64	28	7.19	2.50	4.02	52

in V-type Mixer, ensuring uniform mixing. Cu substrates, 40 × 100 × 3, 20 × 30 × 3 mm<sup>3</sup> cubes were polished with sandpaper and cleaned using Ethanol before coatings were produced.

To analyze the deformability of the powders, the indentation experiments on the cross-sections of the Cu and Cr powders were conducted with a nanoindenter (Nano Indenter II, XP +DCM, MTS, U.S.), under indentation depth of 500 nm. The laser particle size analyzer (LMS-30, Seishin Enterprise, Japan) was used to examine the particle size distribution. And Powder Integrative Characteristic Tester (BT-1000, co-developed by China Tsinghua University and Danodong Bettersize Instrument Co., Ltd., China) was used to measure loose density, tap density, as well as flowability by the Carr index. The morphology of powders, the cross-sectional and surface microstructures of coatings were characterized by scanning electron microscopy (SEM, JEOL JSM-6510A, Japan) with energy dispersive spectrometer (EDS). Porosity (% area) measurements were carried out via an image analysis system (Image-Pro Plus 6.0 software) that analyzes 10 fields at a magnification of 200× or 500× on the sample of polished coating. The Cu powder, Cr powder and Cu-Cr deposits were characterized by x-ray diffraction analysis (D/MAX-RB, Rigaku, Japan). The Vickers hardness was measured on polished and cross-section of the Cu-Cr deposit (without etching) using a microhardness tester (LEICA VMHT 30M, German) at a load of 1000×g. And conductivity of the deposits was measured using an Eddy Current-based Conductivity Meter (FQR-7051, China). The deposits were cut from the substrate to 10 mm × 10 mm × 1 mm cubes by wire cut electrical discharge machining (EDM) and polished before conductivity measurements.

The acceleration process of Cu and Cr particles in the nitrogen in the de Laval nozzle was analyzed using FLUENT software. The stagnation pressure ( $P_0$ ) was 2.0 MPa and the stagnation temperature ( $T_0$ ) was 873 K. Details of the numerical model are described in Ref 18.

## 3. Results and Discussion

### 3.1 Characteristics of the Powders

The particle properties, morphology, size and flowability have an influence on deposition behavior and coatings' quality. Before spraying, the powders were characterized. The results are listed in Table 2. High purity of the original powders ensures that impurities, such as oxygen and nitrogen in the deposits, are in the required range.

The particle velocity and the particle temperature are two of the most important parameters during impact. Both of these parameters have effect on the process of particles adhesion as well as on the properties of the coating. A higher impact velocity generally causes extensive deformation of the particle and the substrate due to higher initial kinetic energy, which is good for coatings formation (Ref 19), while particle preheating improves the plastic deformability of particles by increasing the initial powder temperature. Heating the particles reduces the critical velocity required for deposition. Higher particle velocity and temperature lead to higher coatings densities and reduce porosity. Particle acceleration and heating or cooling in the nozzle are dependent on the particle density, size and morphology.

The morphologies of the powders are shown in Fig. 1. The inset in Fig. 1(a) is an etched cross-section of Cu particle, and the inset in Fig. 1(b) is a cross-section of Cr particle. The Cu powder has spherical morphology and Cr powder has a flake-like shape. The density of Cr is slight less than that of Cu, and the morphologies are different, the loose and tap density of Cr are less than those of Cu, and the flowability of Cr is relatively poor, which affects the feeding and conveying of powders. However, the powder mixture of Cr and Cu were not clogged in the nozzle during the cold spray process. In addition, the size distributions of Cu and Cr shown in Fig. 2(a), are almost

the same. The average diameter size of Cu and Cr are 25 and 28  $\mu\text{m}$ , respectively.

The nozzle inlet was set as the origin in the  $x$  direction. Changes of velocity and temperature of Cu and Cr particles along the nozzle axis are shown in Fig. 3. The particles are accelerated from the throat ( $x=40$  mm) to the exit ( $x=170$  mm). The particle velocity rapidly increases, and then gradually approaches the maximum value at the nozzle exit. Due to the small differences in density and size of Cu and Cr (as shown in Table 2 and Fig. 2), coupled with the assumption that both Cu and Cr particles are spherical with diameters of 25 and 28  $\mu\text{m}$ , respectively, their velocities at the nozzle exit are similar at 440-460 m/s. Smaller particles are accelerated to a higher velocity. When the diameter of Cu particle is 10  $\mu\text{m}$ , the velocity is 620 m/s. In fact, the particle morphology also affects the acceleration process. For non-spherical particle, the higher surface area of the particles increases their drag coefficient to increase the particle velocity. A sphericity of a particle is the ratio of the surface area of a sphere (with the same volume as the given particle) to the surface area of the particle. As for the flake-like morphology of Cr (as shown in Fig. 1), the sphericity is generally set as 0.7. This velocity calculated by simulation was 665 m/s, which is much larger than that of Cu (Ref 20), as shown in Fig. 3.

From the curves of the temperature distribution, the particles are heated by the gas in the convergent section of

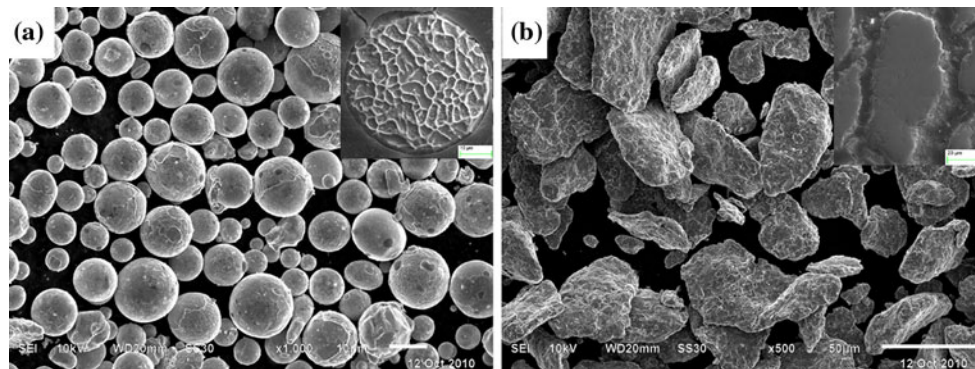


**Fig. 1** SEM images of feedstock powders (a) Cu and (b) Cr, insets are the cross-section of powders

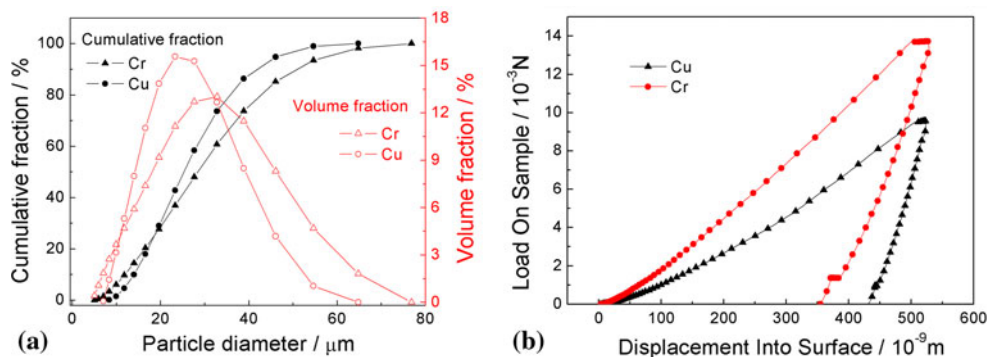


**Fig. 2** (a) Particles diameter distribution of feedstock powders and (b) nanoindent load vs. displacement curves



the nozzle (0-40 mm), the temperature reaches the maximum at the throat ( $x=40$  mm) and decreases steeply in the divergent section (40-170 mm). At the exit ( $x=170$  mm), the temperature of both particles retain a high temperature (680 K). The high Cu particle temperature results in the significant increase of deformability and hence the increase of density of a coating layer.

The different hardness and deformability of Cu and Cr lead to the different deposition characteristic. To analyze the deformability of the powders, the indentation experiments on the cross-sections of the Cu and Cr powders

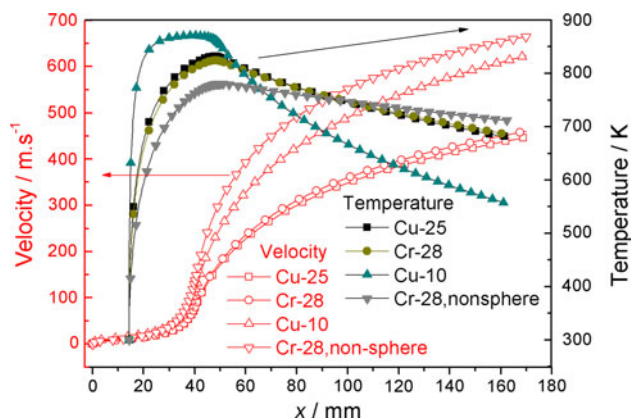


**Fig. 3** Changes of velocity and temperature of Cu and Cr particles along the nozzle axis

were conducted with a nanoindenter. Five tests were conducted to calculate the mean value. The results are listed in Table 2, the nano-hardness of Cu and Cr are  $1.77 \pm 0.12$  and  $2.96 \pm 0.64$  GPa, respectively. The typical nanoindent load vs. displacement curves are shown in Fig. 2(b). Due to high hardness, it is more difficult for the Cr to deform. Therefore, the load on Cr is higher than that on Cu at the depth of 500 nm.

### 3.2 Deposition Behavior of the Wipe Test

Figure 4 demonstrates how the particles bonded to the substrate and the craters created by the Cu+75%Cr composite particles during impact. From Fig. 4(a), several particles bond to the substrate surface (as marked by arrows) while most of them hit the substrate and then detach from the surface, and craters are formed. From Fig. 4(b), almost all of bonded particles are Cu while only a few bonded Cr particles are observed. Simulated result of particle/substrate bond (Ref 9) is shown in Fig. 4(c). Also, the cross-section of bonded Cu particles is shown in Fig. 4(d), in which both particle and substrate undergo extensive plastic deformation. According to the simulated results, the local deformed zone marked by arrows in Fig. 4(d) may experience shear instability, forming a large strain region, nano/micro length-scale mechanical material mixing at the particle/substrate interface, and thus formed a tight bond. The craters created by Cu and Cr were totally different from their morphology. When the spherical Cu particle impacted the substrate, the craters floor were smooth (as shown in Fig. 4b) while the surface of

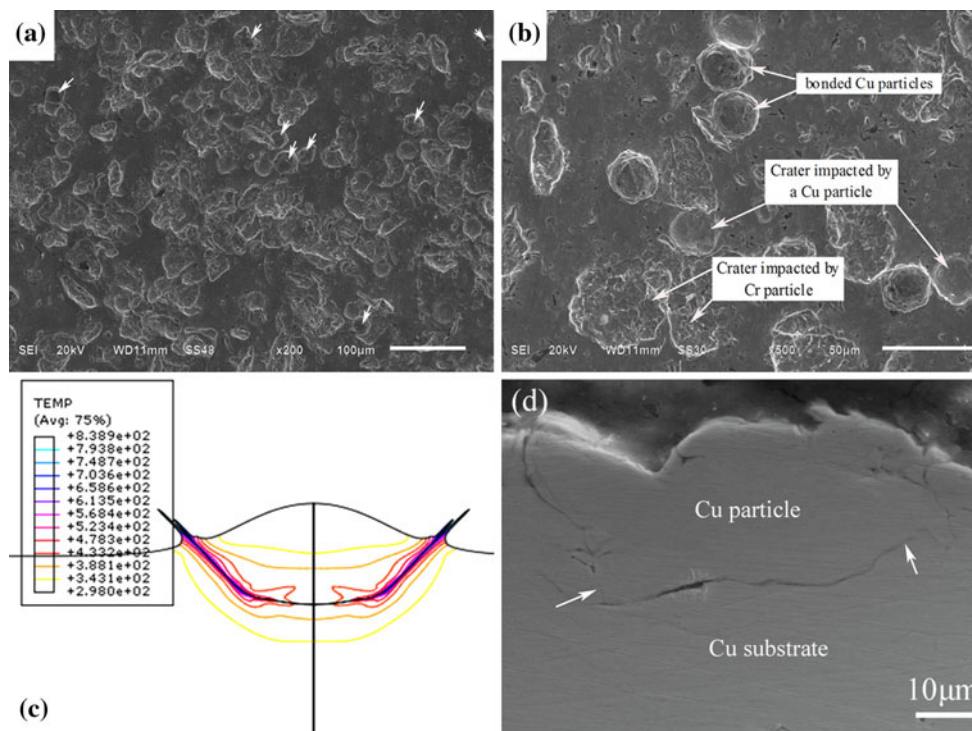


**Fig. 4** Substrate surface impacted by Cu + 75%Cr feedstock powders (a) low magnification, (b) high magnification, (c) simulated results of particle/substrate bond (Ref 9) and (d) a cross section microstructure of single Cu particle/Cu substrate

craters impacted by Cr particles were dimpled, as shown in Fig. 4(b). From Fig. 2(b) and 3, both hardness and velocities of the Cr particles are higher than those of Cu particles. When a Cr particle impacts a Cu substrate, there was less deformation thus the higher kinetic energy was mainly dissipated into plastic deformation and viscous effects/frictional work of the Cu substrate, which led to more intensive deformation and higher strain rate for substrate. The dimpled crater floor was caused by large strain and high strain rate of the substrate.

From what has been discussed above, one can conclude that two types of particles represented different deposition characteristics; the Cu has a much higher bond probability than that of Cr. From Fig. 3, the temperatures of Cu and Cr particles at the nozzle exit are nearly the same, and their density are also similar (Cu,  $8.96 \text{ g/cm}^3$ ; Cr,  $7.2 \text{ g/cm}^3$ ), the difference of deposition, therefore, resulted from the different deformation and velocities of the Cu and Cr particles. The hardness of Cu is relatively low (see Fig. 2b), so plastic deformation easily occurs during impacting. Although the velocity of Cr particles is higher than that of Cu, Cr particles detach from the substrate surface, and craters are formed because they are hard and brittle. The differences in mechanical properties, physical properties, and particle sizes of the composite powders can result in different critical velocities and deposition efficiencies. Therefore, the fraction of each component in the coating can be quite different from that in the original powder mixture (Ref 13, 14, 21).

### 3.3 Surface Microstructure of Composite Deposits

During the cold-sprayed deposition process, particles impact the substrate or the previously deposited particles. Multi-particle interactions, such as tamping, interlocking and extrusion effects, can hinder rebound of the previously deposited particles (Ref 19, 22). The bonding state was analyzed using SEM to investigate the surface microstructure of composite deposits. Figure 5 shows the bonded micro-particles on the deposit surface. The combination of two Cu particles (with  $\sim 25 \mu\text{m}$  in diameter) is shown in Fig. 5(a). The two particles impact deposited layer, and the lower half of particle has undergone severe plastic deformation, while the upper half still remains spherical. A highly magnified morphology is shown in Fig. 5(b). The rebound phenomenon caused two particles split each other, where one can see the disconnected interface. An etched cross-sectional microstructure of Cu-Cr is shown in Fig. 6, spherical Cu particles has been flattened to splats, and the equiaxed grain at the contact interface also has been tripped long. The intense deformed areas are indicated by arrows. According to simulated results (Fig. 4c), these areas have been experienced shear instability. Due to adiabatic shear instability, the out-flowing material jet at the local intensively deformed zones disrupted films on the surface, such as oxides, exposed fresh metal, and provided intimate conformal contact. Local severe deformation at the particle interface brought about a physical bond of fresh metal between Cu

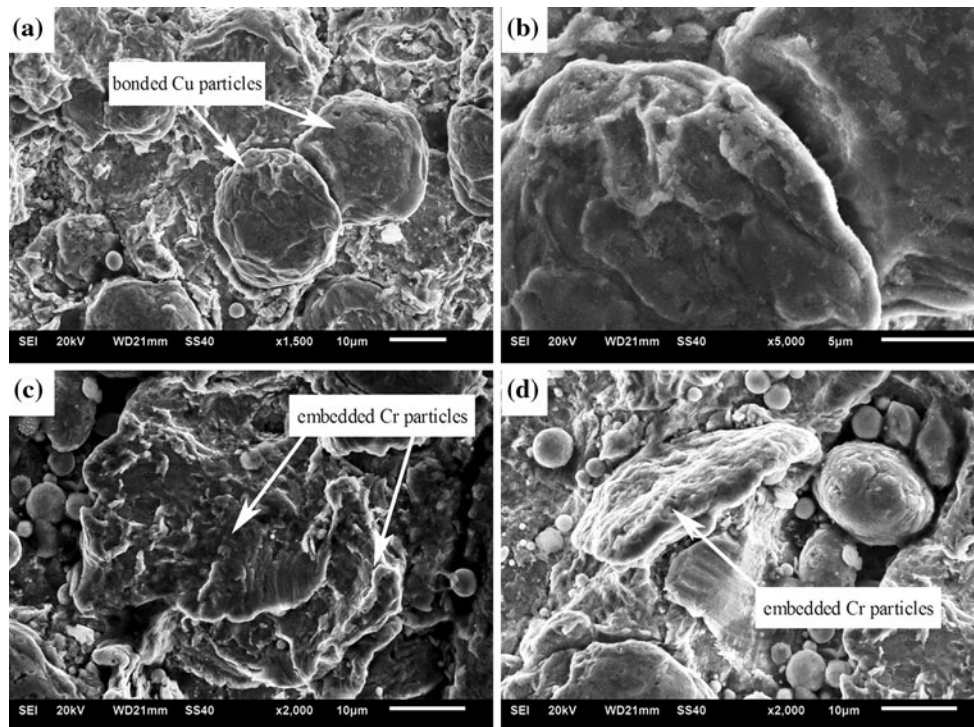


**Fig. 5** SEM morphology of the deposits (a) bonded Cu particles, (b) its high magnification of the interface between the Cu particles, and (c, d) bonded Cr particles



particles. However, Fig. 5(c) and (d) demonstrates the morphologies of the flake shape Cr particles. Two Cr particles in Fig. 5(c) stacked together, no fresh metal bond interface is observed. A Cr flake with less deformation is just embedded in the deposited Cu layer, as shown in Fig. 5(d). Therefore, deposition efficiency of Cr is lower and the content of hard phase Cr in the deposit would be less than in the original powders.

### 3.4 Microstructures and Properties

Figure 7 shows typical cross-sectional microstructures of Cu-Cr composite (not etched) deposited by cold spraying. The images were produced with an SEM in backscattered mode. It can be seen in Fig. 7(a) and (b) that the coating has two distinct regions. One region is a

dark representing Cr, and the other is a light area mostly occupied by the Cu matrix. Clearly, the coating presents a dense microstructure. The porosity measured by analyzing the SEM images is  $0.24 \pm 0.04\%$ . Cr particles are uniformly distributed in the coating. At the interfaces between Cu particles and Cr particles, no obvious voids and cracks are observed in Fig. 7(b).

Cold spraying process can be used to prepare Cu-Cr composite deposits with a high density and uniform distribution of Cr. However, the main problem is how to ensure the proportion of Cr in deposits is identical with the original powder mixture. The difference in particles parameters of Cu and Cr resulted in the low Cr content in the deposits compared to the feedstock. The compositions of deposits were analyzed using analytical SEM with EDS at a magnification of  $200\times$ . A typical EDS result of whole area in Fig. 7(a) is shown in Fig. 7(c), the mean values were calculated from more than five images. In the present work, the changes of Cr content between the powders and the deposits are listed in Table 3. When Cu-50%Cr and Cu-75%Cr are as feedstock, the Cr content in the deposits are  $10.0 \pm 0.74$  and  $15.3 \pm 0.25\%$ , respectively. The reason of low Cr content is that the bond probability of Cr was lower due to the high hardness and poor deformation.

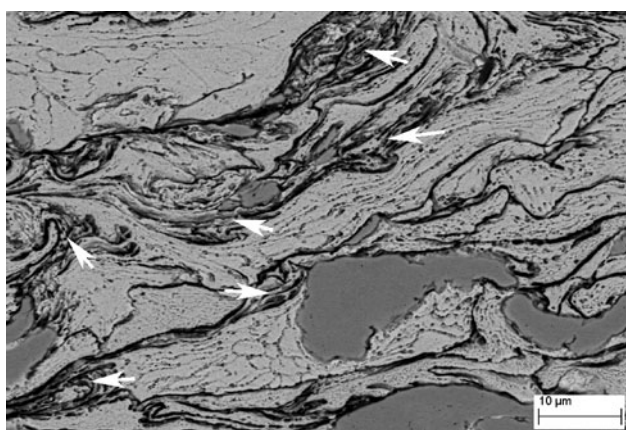


Fig. 6 Etched cross-sectional SEM morphology of the deposits

Table 3 Changes of Cr content between the powders and the deposits

	Cr, wt.% of powders	Cr, wt.% in deposits
Cu-50Cr	50	$10.0 \pm 0.74$
Cu-75Cr	75	$15.3 \pm 0.25$

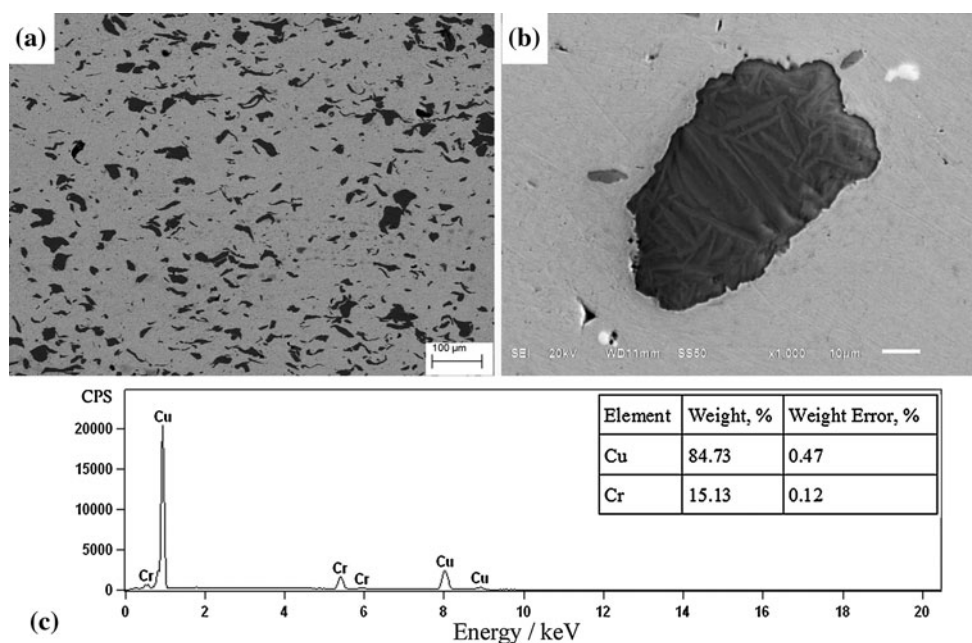
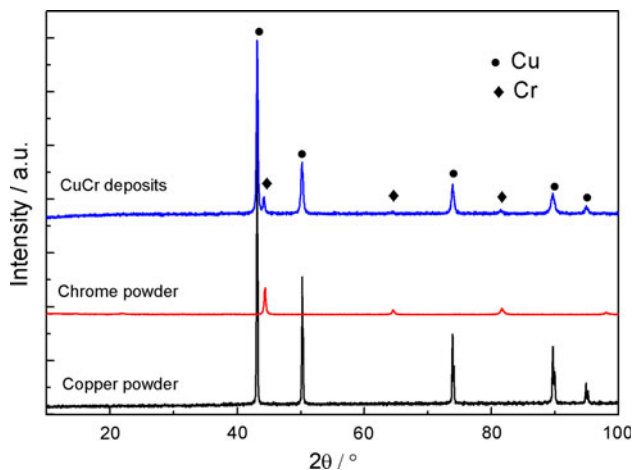


Fig. 7 Microstructure of the Cu/Cr composite deposits by cold spraying (a) low magnification, (b) high magnification and (c) EDS result of whole area in Fig. 7(a)

**Table 4 Comparison of different properties for some processes**

Properties	Industrial standard	Explosive compacted	Coated powders	Cold-sprayed
		Cu-10%Cr (Ref 3)		Cu-15%Cr
Relative density or porosity	Relative density: 95-96%	Relative density: 98.5-98.9%	Relative density: 99.1-99.2%	Porosity: $0.24 \pm 0.039\%$
Hardness (VHN)	100	119	104	$232 \pm 6.5$
Conductivity (%IACS)	55	69.7	84.5	$71.5 \pm 0.73$

**Fig. 8** XRD patterns of feedstock powders and cold-sprayed deposits

The hardness and electrical conductivity were carried out for the Cu-15%Cr deposits. The properties are compared with those of Cu-10%Cr (Ref 3) in Table 4. The Cu-10%Cr powder mixtures were mechanically alloyed, and then were subjected to different processing routes: (a) explosive compaction and (b) coating by Cu followed by uni-axial cold compaction. The hardness of Cu-15%Cr in present work is  $232 \pm 6.5$  HV, much higher than the others. The conductivities of copper substrates and Cu-Cr deposits were measured and five measurements were carried. The values of deposits are 70.93, 70.93, 71.28, 72.67, 71.80 %IACS, respectively, and the mean electrical conductivity is  $71.5 \pm 0.73$  %IACS, superior to that of explosive compacted composite (69.7 %IACS), while the conductivity of copper substrate is 90.8 %IACS. Additionally, the composite is also dense. The properties of Cu-15%Cr composite met industrial standard, were better than the composite prepared by explosive compaction. Figure 8 shows the XRD patterns of original powders and deposits. The results indicate no obvious oxidation of Cu-Cr deposits. The deposit did not form a new phase during cold spraying process, only mechanical mixing of Cu and Cr was observed.

Therefore, it is feasible to prepare uniform and dense Cu-Cr alloy contact materials by cold spraying. But further detail researches must be done to improve the Cr content in the deposits and the coating performances, such as pretreatment of feedstock powders, optimization of cold spraying, and so on.

## 4. Conclusions

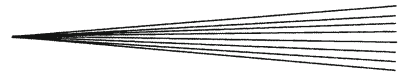
Cu-Cr composite was deposited using cold spray process, the bonding of single particle/substrate and the surface and inter-particle interface of the deposit were analyzed. Particle parameters, such as morphology, size distribution and deformability, resulted in different deposition behavior. For Cu, plastic deformation easily occurred, when a Cu particle impacted a substrate or previously deposited layer, both of the particle and the substrate had undergone extensive deformation, resulting in the higher bond probability. Although the flake shape improved the velocity of Cr particles to reach a higher value than that of Cu, Cr particles had lower bond probability because it was hard and brittle. Cr particles were embedded in former Cu particles. The porosity, hardness and electrical resistivity for the Cu-15%Cr deposits were  $0.24 \pm 0.039\%$ ,  $232 \pm 6.5$  HV, and  $71.5 \pm 0.73$  %IACS, respectively. These properties met industrial standard, superior to the composite prepared by explosive compaction. Therefore, it is feasible that cold spraying can be considered as a suitable method for Cu-Cr composite.

## Acknowledgments

This work was financially supported by the National Natural Science Foundation of China (Nos. 50871019 and 50874009) and State Key Laboratory for Advanced Metals and Materials, University of Science and Technology Beijing.

## References

- W. Li, R.L. Thomas, and R.K. Smith, Effects of Cr Content on the Interruption Ability of CuCr Contact Materials, *IEEE Trans. Plasma Sci.*, 2001, **29**(5), p 744-748
- P.G. Slade, Advances in Material Development for High Power, Vacuum Interrupter Contacts, *IEEE Trans. Compon. Packag. Manuf. Technol. A*, 1994, **17**(1), p 96-106
- I. Lahiri and S. Bhargava, Compaction and Sintering Response of Mechanically Alloyed Cu-Cr Powder, *Powder Technol.*, 2009, **189**(3), p 433-438
- C. Zhang, Y. Wang, Z. Yang, Y. Guo, and D. Bingjun, Microstructure and Properties of Vacuum Induction Melted CuCr25 Alloys, *J. Alloy. Compd.*, 2004, **366**(1-2), p 289-292
- Z.M. Zhou, Y.P. Wang, J. Gao, and M. Kolbe, Microstructure of Rapidly Solidified Cu-25wt.%Cr Alloys, *Mater. Sci. Eng. A*, 2005, **398**(1-2), p 318-322
- X. Wang, J. Zhao, and J. He, Investigation on the Microstructure and Mechanical Properties of the Spray-Formed Cu-Cr Alloys, *Mater. Sci. Eng. A*, 2007, **460-461**(7), p 69-76



7. K.T. Chiang, P.D. Krotz, and J.L. Yuen, Blanching Resistant Cu-Cr Coating by Vacuum Plasma Spray, *Surf. Coat. Technol.*, 1995, **76-77**(Part 1), p 14-19
8. A. Papyrin, Cold Spray Technology, *Adv. Mater. Process.*, 2001, **159**(9), p 49-51
9. G. Bae, Y. Xiong, S. Kumar, K. Kang, and C. Lee, General Aspects of Interface Bonding in Kinetic Sprayed Coatings, *Acta Mater.*, 2008, **56**(17), p 4858-4868
10. H. Assadi, F. Gartner, T. Stoltenhoff, and H. Kreye, Bonding Mechanism in Cold Gas Spraying, *Acta Mater.*, 2003, **51**(15), p 4379-4394
11. V. Luzin, K. Spencer, and M.X. Zhang, Residual Stress and Thermo-Mechanical Properties of Cold Spray Metal Coatings, *Acta Mater.*, 2011, **59**(3), p 1259-1270
12. S.B. Kang, H.K. Kang, and K. Euh, Processing and Microstructures of Tungsten/Copper Composites Produced by Plasma Spray and Cold Spray, *Mater. Sci. Forum*, 2005, **475-479**(PRICM 5), p 475-479, 945
13. H.K. Kang and S.B. Kang, Tungsten/Copper Composite Deposits Produced by a Cold Spray, *Scr. Mater.*, 2003, **49**(12), p 1169-1174
14. S. Shin, S. Yoon, Y. Kim, and C. Lee, Effect of Particle Parameters on the Deposition Characteristics of a Hard/Soft-Particles Composite in Kinetic Spraying, *Surf. Coat. Technol.*, 2006, **201**(6), p 3457-3461
15. H.T. Wang, C.J. Li, G.J. Yang, and C.X. Li, Cold Spraying of Fe/Al Powder Mixture: Coating Characteristics and Influence of Heat Treatment on the Phase Structure, *Appl. Surf. Sci.*, 2008, **255**(5), p 2538-2544
16. T. Novoselova, P. Fox, R. Morgan and N. W. O, Experimental study of titanium/aluminium deposits produced by cold gas dynamic spray, *Surf. Coat. Technol.*, 2006, **200**(8), 2775-2783
17. D. Pantelis, K. Triantou, C. Sarafoglou, D. Christoulis, F. Borit, V. Guipont, and M. Jeandin, Microstructural Study of Copper and Copper/Alumina Composite Coatings Produced by Cold Spray Process, *Adv. Mater. Res.*, 2010, **89-91**(THERMEC 2009 Supplement), p 556-561
18. W.Y. Li, C.J. Li, H.T. Wang, C.X. Li, and H.S. Bang, Measurement and Numerical Simulation of Particle Velocity in Cold Spraying, *J. Therm. Spray Technol.*, 2006, **15**(4), p 559-562
19. G. Bae, S. Kumar, S. Yoon, K. Kang, H. Na, H. Kim, and C. Lee, Bonding Features and Associated Mechanisms in Kinetic Sprayed Titanium Coatings, *Acta Mater.*, 2009, **57**(19), p 5654-5666
20. S. Kumar, H. Na, V. Selvarajan, and C. Lee, Influence of Metal Powder Shape on Drag Coefficient in a Spray Jet, *Curr. Appl. Phys.*, 2009, **9**(3), p 678-682
21. S. Shin, Y. Xiong, Y. Ji, H.J. Kim, and C. Lee, The Influence of Process Parameters on Deposition Characteristics of a Soft/Hard Composite Coating in Kinetic Spray Process, *Appl. Surf. Sci.*, 2008, **254**(8), p 2269-2275
22. G. Bae, K. Kang, J. Kim, and C. Lee, Nanostructure Formation and Its Effects on the Mechanical Properties of Kinetic Sprayed Titanium Coating, *Mater. Sci. Eng. A*, 2010, **527**(23), p 6313-6319